

Stabilization of Kinetic Internal Kink Mode by Electron Diamagnetic Effect

NAITOU Hiroshi, KOBAYASHI Toshimitsu¹, KURAMOTO Takehisa, TOKUDA Shinji² and MATSUMOTO Taro²
Department of Electrical and Electronic Engineering, Yamaguchi University, Tokiwadai 2-16-1, Ube 755-8611, Japan

¹*Integrated Information Processing Center, Yamaguchi University, Tokiwadai 2-16-1, Ube 755-8611, Japan*

²*Department of Fusion Plasma Research, Naka Fusion Research Establishment, Japan Atomic Energy Research Institute, Naka Ibaraki 311-0193, Japan*

(Received: 8 December 1998 / Accepted: 13 May 1999)

Abstract

Effects of density gradients on the $m = 1$ (poloidal mode number) and $n = 1$ (toroidal mode number) kinetic internal kink mode are studied numerically by the linear version of GRM3F-CY code which is the three-field gyro-reduced-MHD code in the cylindrical coordinates. In order to resolve the collisionless electron skin depth, d_e , near the rational surface in the realistic parameters of present day large tokamaks in which d_e/a (a is a minor radius of a plasma) is less than 10^{-3} , GRM3F-CY accumulates the meshes near the $q = 1$ surface. For $\omega_{*e} \leq 2\gamma_0$, where ω_{*e} and γ_0 are electron diamagnetic angular frequency and the growth rate for the uniform density, respectively, the growth rate reduces drastically as ω_{*e} increases. However very weak instability remains for $\omega_{*e} > 2\gamma_0$. This residual instability becomes large if d_e/a is greater than the order of 10^{-3} .

Keywords:

internal kink mode, gyrokinetic theory, sawtooth oscillation, tokamak, collisionless magnetic reconnection

1. Introduction

To understand the kinetic modification of MHD modes in present day and future high temperature large tokamaks, it is inevitable to develop simulation codes based on extended MHD models. We have developed gyrokinetic particle code (GYR3D) [1,2], gyro-reduced-MHD code (GRM3D-2F) [3], and Hybrid code (Hybrid3D) [4] to study kinetic modification of MHD modes in a tokamak. These codes have been coded for the rectangular mesh and fast fourier transformation technique is used. The linear and nonlinear development of the $m = 1$ (poloidal mode number) and $n = 1$ (toroidal mode number) kinetic internal kink mode are simulated successfully. However it has been felt that the cylindrical model with mode expansions in toroidal and

poloidal angles would be more powerful to simulate realistic plasmas. The mesh accumulation technique in the radial direction can be used for the cylindrical code. For example, in order to simulate a $m = 1$ and $n = 1$ kinetic internal kink mode, we must resolve the collisionless electron skin depth, $d_e = c/\omega_{pe}$ (c is the speed of light in vacuum and ω_{pe} is the electron plasma angular frequency), around the $q = 1$ (q is the safety factor) surface. For the parameters of present day large tokamaks, d_e/a (a is a minor radius of a plasma) is less than 10^{-3} . By accumulating radial meshes around the $q = 1$ surface, we can simulate the physics including the thin inertial layer by using the moderate number of meshes. As the first step to build the series of cylindrical codes,

Corresponding author's e-mail: naitou@plasma.eee.yamaguchi-u.ac.jp

we developed linear version of the GRM3F-CY code which is based on the three field gyro-reduced-MHD model. This paper treats the stabilization of kinetic internal kink mode with the density gradients by using the linearized version of GYM3F-CY code.

2. Basic Equations

We assume a uniform (toroidal) magnetic field, $\mathbf{B} = B_0 \mathbf{b}$, where \mathbf{b} is the unit vector in the z direction. The five field gyro-reduced MHD model [5] was derived by moment equations of the gyro-kinetic equations [6]. By assuming $\Gamma_i = 0$ (ion flux along the magnetic field), the five field model reduces to the three field model which is equivalent to the subset of four field model by Aydemir [7]:

$$\frac{\partial}{\partial t} (\nabla_{\perp}^2 \phi) = - \frac{\mathbf{b} \times \nabla \phi}{B_0} \cdot \nabla (\nabla_{\perp}^2 \phi) - v_A^2 \mathbf{b}^* \cdot \nabla (\nabla_{\perp}^2 A_z), \quad (1)$$

$$\frac{\partial}{\partial t} A_z = - \mathbf{b}^* \cdot \nabla \phi + d_e^2 \frac{d}{dt} (\nabla_{\perp}^2 A_z) + \frac{T_e}{n_{e0} e} \mathbf{b}^* \cdot \nabla n_e, \quad (2)$$

$$\frac{\partial}{\partial t} n_e = - \frac{\mathbf{b} \times \nabla \phi}{B_0} \cdot \nabla n_e - \frac{1}{e \mu_0} \mathbf{b}^* \cdot \nabla (\nabla_{\perp}^2 A_z), \quad (3)$$

where ϕ is the electrostatic potential, A_z is the z component of the vector potential, n_e is the electron density, v_A is the Alfvén velocity, T_e is the electron temperature, n_{e0} is the average electron density, e is the electron charge, μ_0 is the permeability in vacuum, \mathbf{b}^* is the unit vector of the magnetic field, $\mathbf{b}^* = \mathbf{b} + (\nabla A_z \times \mathbf{b})/B_0$, and d/dt is the convective derivative defined by $d/dt = \partial/\partial t + [(\mathbf{b} \times \nabla \phi)/B_0] \cdot \nabla$. Eq.(1) represents the vortex equation while generalized Ohm's law in the direction parallel to the magnetic field is described by Eq.(2). Eq.(3) represents continuous equation of the electron density.

To derive Eq.(2), we adopted the isothermal model as $p_e = n_e T_e$ and $T_e = \text{constant}$. Because we are based on the lowest order gyrokinetic equations, the ion polarization response ($\omega_{pi}^2/\omega_{ci}^2 \nabla_{\perp}^2 \phi$, where ω_{pi} is the ion plasma angular frequency and ω_{ci} is the ion cyclotron angular frequency) in the gyrokinetic Poisson equation is defined for the average density. Therefore, $v_A = c \omega_{ci}/\omega_{pi}$ is constant in space. The total energy is conserved for this three field model.

3. Effects of Density Gradients

The stability of $m = 1$ and $n = 1$ kinetic internal kink mode is studied by the linearized version of

GRM3F-CY code which simulates the time evolution of the unstable mode as a initial value problem. We assume a cylinder with a minor radius of a and a height of $L_z = 2\pi R$ (R is a major radius) surrounded by a perfectly conducting wall. Periodic boundary condition is used in the z direction. GRM3F-CY utilizes the following normalization: $z/L_z \rightarrow z$, $r/a \rightarrow r$, $tv_A/L_z \rightarrow t$, $A_z L_z/(a^2 B_0) \rightarrow A_z$, $\phi L_z/(v_A a^2 B_0) \rightarrow \phi$, $n_e L_z/(n_{e0} d_e) \rightarrow n_e$. The normalized equations include only two parameters, d_e/a and ρ_s/a , where $\rho_s = \sqrt{T_e/m_i}/\omega_{ci}$ (m_i is the ion mass) is the ion Larmor radius estimated by the electron temperature.

We selected the parameters close to the present day large tokamaks: $a = 1$ [m], $R = 3$ [m], $n_{e0} = 10^{20}$ [m⁻³], magnetic field strength of $B = 5$ [Tesla], and $T_e = 10$ [keV]. For such a tokamak with deuteron discharge, $d_e/a = 5.315 \times 10^{-4}$ and $\rho_s/a = 2.891 \times 10^{-3}$. The profile of the safety factor is

$$q(r) = q_0 \left[1 - 4(1 - q_0) \left(\frac{r}{a} \right)^2 \right]^{-1}, \quad (4)$$

where $q_0 = 0.85$ is the safety factor at the magnetic axis. Note that $q(a/2) = 1.0$ and $q(a) = 2.125$. The equilibrium density profile is chosen as

$$n(r) = n_0 \left(1 - \varepsilon_n \tanh \frac{r - r_0}{l_n} \right), \quad (5)$$

where $r_0 = a/2$, $l_n = 0.16 a$, and ε_n is used to change the density gradients.

Figure 1 shows the summary of the effects of density gradients on the growth rate. The electron

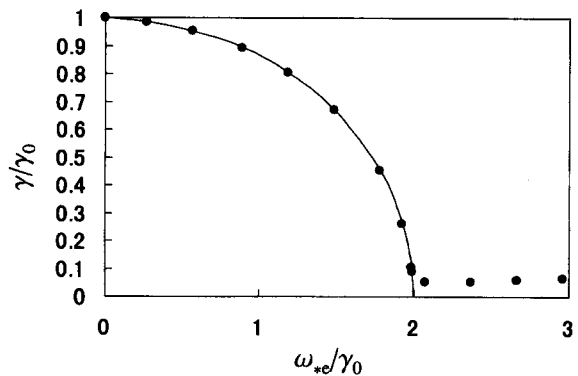


Fig. 1 The normalized growth rate γ/γ_0 versus ω_{*e}/γ_0 , where γ_0 is the growth rate of kinetic internal kink mode without a density gradient and ω_{*e} is the electron diamagnetic angular frequency estimated at the $q = 1$ rational surface. The curve written in the figure is $\gamma/\gamma_0 = \sqrt{1 - (\omega_{*e}/2\gamma_0)^2}$.

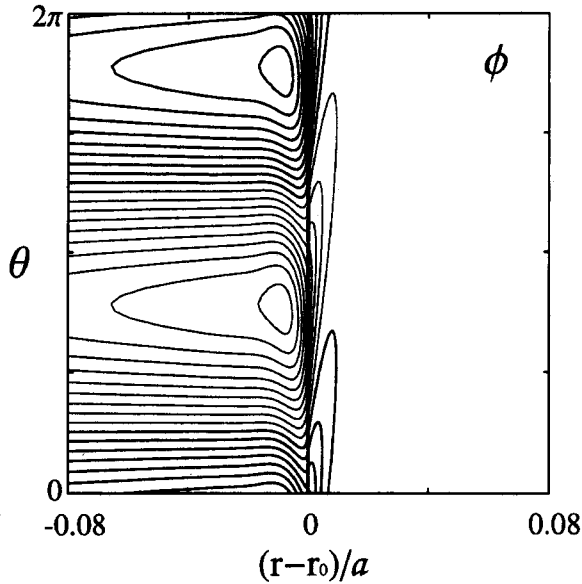


Fig. 2 The contour plot of ϕ around the $q = 1$ magnetic surface at $r = r_0$ in the $r - \theta$ coordinates. The case with a density gradient of $\varepsilon_n = 0.1414$.

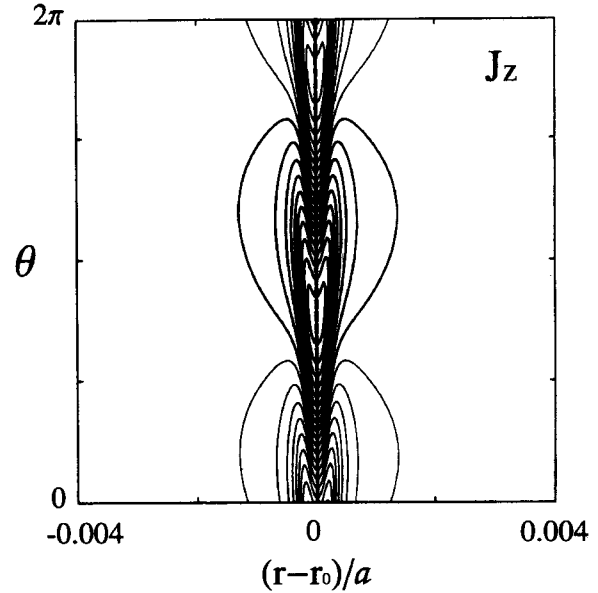


Fig. 3 The contour plots of J_z around the $q = 1$ magnetic surface at $r = r_0$ in the $r - \theta$ coordinates. The case with a density gradient of $\varepsilon_n = 0.1414$.

diamagnetic frequency is defined by $\omega_{*e} = (T_e / reB_0 n_e) dn_e / dr$. We have used 256 nonuniform grid points in the radial direction. The growth rate for the uniform density is $\gamma_0 = 5.84 \times 10^{-3} v_A / L_z$; the characteristic time for the instability, $1/\gamma_0$, is about 417 μsec . The curve in the figure represents the simple theory of ω_{*e} stabilization [8]: $\gamma = \gamma_0 [1 - (\omega_{*e}/2\gamma_0)^2]^{\frac{1}{2}}$, where we estimated ω_{*e} at $r = r_0$. For $\omega_{*e} \leq 2\gamma_0$, the ω_{*e} dependence of the growth rate agrees very well with the theory; γ reduces drastically as ω_{*e} increases. However very weak instability remains for $\omega_{*e} > 2\gamma_0$. We made a convergence study by increasing meshes, and found that the amplitude of this residual instability is about 5 per cents of γ_0 . This residual instability becomes large if d_e/a is greater than the order of 10^{-3} .

Figure 2 and 3 show ϕ and J_z (current density along the magnetic field) profiles around the $q = 1$ surface for $\varepsilon_n = 0.1414$ ($\omega_{*e}/\gamma_0 = 1.48$). These mode patterns move in the direction of the electron diamagnetic drifts. Figure 4 shows the potential profile around the $q = 1$ surface for $\varepsilon_n = 0.1895$ ($\omega_{*e}/\gamma_0 = 1.98$) which is very close to the theoretical limit of $\omega_{*e}/\gamma_0 = 2$. The radial extent of the potential perturbation becomes large as the density gradient increases.

4. Conclusions and Discussion

Effects of density gradients on the $m = 1$ (poloidal mode number) and $n = 1$ (toroidal mode number) kinetic

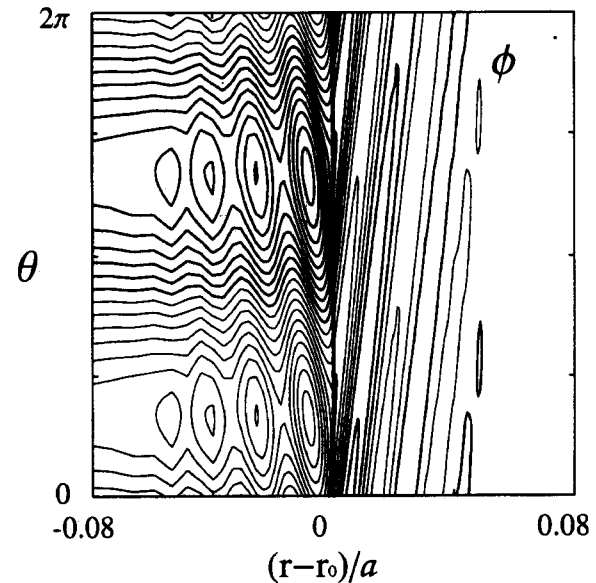


Fig. 4 The contour of ϕ around the $q = 1$ magnetic surface at $r = r_0$ in the $r - \theta$ coordinates. The case with a density gradient of $\varepsilon_n = 0.1895$.

internal kink mode are studied numerically by the linearized version of GRM3F-CY code which is the three-field gyro-reduced-MHD code in the cylindrical coordinates. In order to resolve the collisionless electron

skin depth in the realistic parameters of present day large tokamaks, GRM3F-CY accumulates meshes around the $q = 1$ rational surface. We have selected $d_e = 5.315 \times 10^{-4}$ and $\rho_s = 2.891 \times 10^{-3}$. Although very small instability remains for $\omega_{*e} > 2\gamma_0$, the ω_{*e} stabilizing effect following the simple theory is observed for $\omega_{*e} \leq 2\gamma_0$.

One explanation of the ω_{*e} stabilization is that, for the Ohm's law along the magnetic field, there is no direct effects of density gradients at the $q = 1$ rational surface because $k_{\parallel} = 0$. Hence, for the negative and positive current layer at the $q = 1$ surface, there appears a effective strong shear flow inside the current layer which can destroy the current layer profile characteristic to the unstable kinetic internal kink mode. The another explanation of the ω_{*e} stabilization is the energy extraction from the unstable region by the drift wave. The stabilization is, hence, effective only if there is a sufficient space around the $q = 1$ rational surface so that the drift wave can propagate in the radial directions. (This stabilization is not so effective if d_e/a is greater than the order of 10^{-3} .) Although ion Landau damping was not included in this study, it may be possible that the inclusion of ion Landau damping may increase the stabilizing effects of the drift wave propagating outside of the $q = 1$ surface.

It will be interesting to study nonlinear behavior of the residual instability, since this instability has both

characteristics, electrostatic drift wave and internal kink mode. Thus the development of the nonlinear version of GRM3F-CY code is our project in the near future.

Acknowledgement

The authors are grateful to Professor Osamu Fukumasa, Yamaguchi University, Dr. M. Azumi, JAERI, and Professors T. Sato and T. Kamimura, National Institute for Fusion Science for supporting their works.

References

- [1] H. Naitou, K. Tsuda, W.W. Lee and R.D. Sydora, *Phys. Plasmas* **2**, 4257 (1995).
- [2] H. Naitou, T. Sonoda, S. Tokuda and V.K. Decyk, *Journal of Plasma and Fusion Research* **72**, 259 (1996).
- [3] H. Naitou, H. Kitagawa and S. Tokuda, *Journal of Plasma and Fusion Research* **73**, 174 (1997).
- [4] S. Tokuda, H. Naitou and W.W. Lee, *Journal of Plasma and Fusion Research* **74**, 44 (1998).
- [5] W.W. Lee, *reports presented at US-Japan Workshop on Plasma Modeling with MHD and Particle Simulation*, Sep. 25-26, 161 (1987).
- [6] T.S. Hahm, W.W. Lee and A. Brizard, *Phys. Fluids* **31**, 1940 (1988).
- [7] A.Y. Aydemir, *Phys. Fluids* **B4**, 3469 (1992).
- [8] F. Porcelli, *Phys. Rev. Lett.* **28**, 425 (1991).